Paper 51

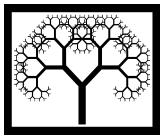

Proceedings of the Eleventh International Conference
on Computational Structures Technology,
B.H.V. Topping, (Editor),
Civil-Comp Press, Stirlingshire, Scotland

Thermal Postbuckling Behaviour of Rectangular Functionally Graded Plates using the Finite Strip Method

H.R. Ovesy[1], S.A.M. Ghannadpour[2] and M. Nassirnia[1]
[1] Department of Aerospace Engineering and
Centre of Excellence in Computational Aerospace Engineering
Amirkabir University of Technology, Tehran, Iran
[2] Aerospace Engineering Department, Faculty of New Technologies
and Engineering, Shahid Beheshti University G.C., Tehran, Iran

Abstract

Description is given of semi-analytical finite strip method applied for analysing the postbuckling behaviour of functionally graded rectangular plates under thermal loadings. The material properties of these plates are assumed to vary continuously through the thickness of the plate, according to the power product form of thickness coordinate variable *z*. The formulations are based on the classical plate theory and the concept of the principle of the minimum potential energy. The Newton-Raphson method is used to solve the non-linear equilibrium equations. A range of applications are described and the numerical results are compared to the available results, wherever possible.

Keywords: postbuckling, thermal loading, classical plate theory, finite strip method, functionally graded material.

1 Introduction

Functionally graded materials (FGMs) are those in which the volume fractions of two or more constituents are varied continuously as a function of position along certain dimension of the plate to achieve a required function. By gradually varying the volume fraction of constituent materials, their mechanical properties exhibit a smooth and continuous change from one surface to the other one. The ceramic constituent of the material provides the high-temperature resistance due to its low thermal conductivity. Thus FGMs have received considerable attention as one of advanced inhomogeneous composite materials in many engineering applications by eliminating interface problems and alleviating thermal stress concentrations. Most of the researches on FGMs have been restricted to thermal stress analysis, fracture mechanics, and optimization. However, very little work has been done to consider

the buckling, post buckling and vibration behavior of structures constructed of FGM.

Since Finite Strip Method (FSM) is well suited to the accurate and efficient analysis of both single rectangular plates and complicated prismatic plate structures, the first two authors of the current paper and their co-workers have made several contributions by developing different versions of finite strip methods, namely full-energy semi-analytical FSM [1],[2], full-energy spline FSM [1], semi-energy FSM [2] and exact FSM [3].

Ge et al. investigated postbuckling behaviour of composite laminated plates with the aid of the B-spline finite strip method under the combination of temperature load and applied uniaxial mechanical stress [4]. Liew et al. examined the postbuckling behavior of functionally graded material FGM rectangular plates that are integrated with surface-bonded piezoelectric actuators and are subjected to the combined action of uniform temperature change, in-plane forces, and constant applied actuator voltage [5]. Sohn et al. worked on static and dynamic stabilities of functionally graded panels based on the first-order shear deformation theory which are subjected to combined thermal and aerodynamic loads. They derived equations of motion by the principle of virtual work and numerical solutions were obtained by a finite element method. In addition, they utilized the Newton–Raphson method to get solutions of the nonlinear governing equations [6]. The authors of the current work developed the S-a FSM for analyzing the buckling behavior of rectangular FGM plates under thermal loadings by incorporating the total potential energy minimization and solving the corresponding eigenvalue problem [7].

In the current research, the application of the FSM is extended to the analysis of postbuckling behavior of functionally graded plates subjected to the three types of thermal loadings, i.e. uniform temperature rise, tent-like temperature distribution and nonlinear temperature change across the thickness. Material properties are assumed to be graded in the thickness direction according to a simple power law distribution in terms of the volume fractions of the constituents. For simplification, the properties are assumed to be temperature-independent.

2 Theoretical Developments

In this section, the fundamental elements of the developed theory of the S-a FSM are outlined. It should be noted that throughout the theoretical developments of this paper, an initially flat plate based on the classical plate theory (CPT) is assumed.

Suppose a rectangular FGP whose longitudinal and transverse dimensions are A and B, respectively. This plate can be divided into several strips called Functionally Graded Strips (FGS) while, as illustrated in Figure 1, they are laid parallel to one another and to the longitudinal edges of the plate.

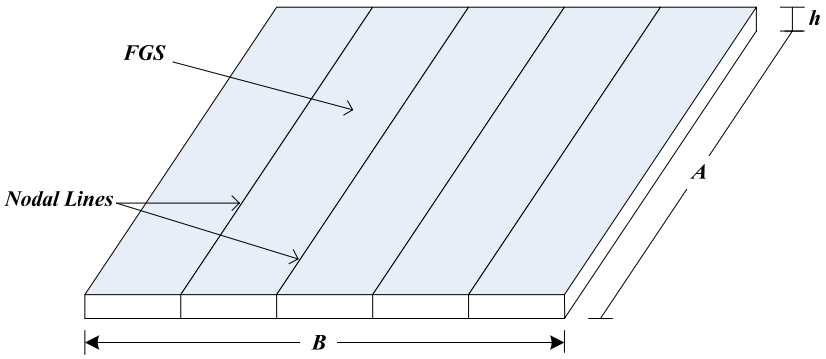

Figure 1. Discretization of a rectangular FGP

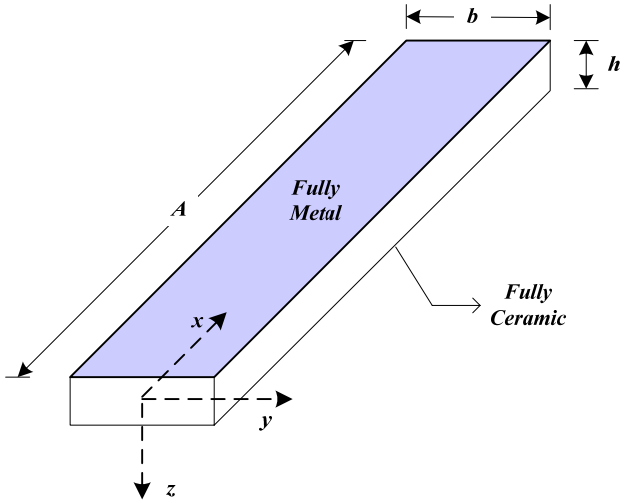

Figure 2. A Typical FGS

It is noted that a single FGS (shown in Figure 2.) forms part of a rectangular FGP of length A (i.e. the same length as that of a strip) and width b (with $B \geq b$). The composition is assumed to vary in such a way that the upper surface of the strip is completely metal (designated by surface m at $z = -h/2$), whereas the lower surface is fully ceramic (designated by surface c at $z = h/2$). Thus, it is assumed that the material properties of the FGS such as the modulus of elasticity E, shear modulus G, thermal expansion coefficient α and thermal conduction coefficient K are changed in the thickness direction z by a function $\vartheta(z)$ which is introduced by power law variations of material properties distribution as

$$\vartheta(z) = \vartheta_{cm}\left(\frac{z}{h} + \frac{1}{2}\right)^{n} + \vartheta_{m} \tag{1}$$

while Poisson's ratio v is assumed to be constant. In Equation (1), ϑ_m and ϑ_c denote values of the variables at surface m and surface c of the strip, respectively

and $\vartheta_{cm} = \vartheta_c - \vartheta_m$.

Moreover, in the above equation, the term $(z/h + 1/2)^n$ is known as the volume fraction of the ceramic phase, and n (volume fraction index) is non-negative real value indicating the material variation profile through the thickness direction.

As a result of the CPT assumption, the Kirchhoff normalcy condition is incorporated, and thus:

$$\begin{aligned} \overline{u}(x,y,z) &= u(x,y) - z\frac{\partial w(x,y)}{\partial x} \\ \overline{\upsilon}(x,y,z) &= \upsilon(x,y) - z\frac{\partial w(x,y)}{\partial y} \\ \overline{w}(x,y,z) &= w(x,y) \end{aligned} \tag{2}$$

where $\overline{u}, \overline{\upsilon}$ and $\overline{w}$ are components of displacement at a general point, whilst u, υ and w are similar components at the middle surfaces $(z = 0)$.

Using Equation (2) in the Green's expressions for the in-plane non-linear strains and neglecting lower-order terms in a manner consistent with the usual Von-Karman assumptions incorporated with the thermal effects gives the following expressions for strains at a general point:

$$\varepsilon_m = \overline{\varepsilon} - \varepsilon_T = \varepsilon_l + \varepsilon_{nl} + z\psi - \varepsilon_T \tag{3-a}$$

where ε_m and ε_T are mechanical and thermal strains, respectively, and

$$\varepsilon_l = \begin{Bmatrix} \dfrac{\partial u}{\partial x} \\ \dfrac{\partial \upsilon}{\partial y} \\ \dfrac{\partial u}{\partial y} + \dfrac{\partial \upsilon}{\partial x} \end{Bmatrix}, \quad \varepsilon_{nl} = \begin{Bmatrix} \dfrac{1}{2}\left(\dfrac{\partial w}{\partial x}\right)^2 \\ \dfrac{1}{2}\left(\dfrac{\partial w}{\partial y}\right)^2 \\ \dfrac{\partial w}{\partial x}\dfrac{\partial w}{\partial y} \end{Bmatrix}, \quad \psi = \begin{Bmatrix} -\dfrac{\partial^2 w}{\partial x^2} \\ -\dfrac{\partial^2 w}{\partial y^2} \\ -2\dfrac{\partial^2 w}{\partial x \partial y} \end{Bmatrix} \tag{3-b}$$

$$\varepsilon_T = \alpha(z).\Delta T(x,y,z)\begin{Bmatrix} 1 \\ 1 \\ 0 \end{Bmatrix}$$

where $\alpha(z)$ is thermal expansion coefficient and $\Delta T(x,y,z) = T(x,y,z) - T_{ref}$ is applied temperature change in Kelvin. It is noted that T_{ref} is an initial temperature which is used as a reference. In the case of non-uniform thermal loading for FG plates, T_{ref} is considered to be equal to the temperature at the metal surface of the plate (i.e. T_m) which is kept constant throughout the analysis. In the presence of a temperature loading and on the assumption that the plate is in a state of plane stress,

the stress–strain relationship at a general point for the plate becomes:

$$\begin{Bmatrix}\sigma_x\\ \sigma_y\\ \sigma_{xy}\end{Bmatrix}=\begin{bmatrix}Q_{11} & Q_{12} & Q_{16}\\ Q_{21} & Q_{22} & Q_{26}\\ Q_{61} & Q_{62} & Q_{66}\end{bmatrix}\left(\begin{Bmatrix}\overline{\varepsilon}_x\\ \overline{\varepsilon}_y\\ \overline{\gamma}_{xy}\end{Bmatrix}-\begin{Bmatrix}\alpha(z)\times\Delta T(x,y,z)\\ \alpha(z)\times\Delta T(x,y,z)\\ 0\end{Bmatrix}\right) \tag{4}$$

where Q_{ij} $(i,j=1,2,6)$ form the reduced stiffness matrix Q.

By the use of Equations (3) and (4) and appropriate integration through the thickness, the constitutive equations for a FGS can be derived as:

$$\begin{Bmatrix}N_x\\ N_y\\ N_{xy}\\ M_x\\ M_y\\ M_{xy}\end{Bmatrix}=\int_{-h/2}^{h/2}\begin{Bmatrix}\sigma_x\\ \sigma_y\\ \tau_{xy}\\ z\sigma_x\\ z\sigma_y\\ z\tau_{xy}\end{Bmatrix}.dz=\begin{bmatrix}[E_1] & [E_2]\\ [E_2] & [E_3]\end{bmatrix}\times\begin{Bmatrix}\{\varepsilon\}\\ \{\psi\}\end{Bmatrix}-\begin{Bmatrix}\{N^T\}\\ \{M^T\}\end{Bmatrix} \tag{5}$$

where $\{N^T\}$ and $\{M^T\}$ are membrane and bending matrices due to the thermal loading, respectively. In the above equation, N_x, N_y and N_{xy} are the membrane direct and shearing stress resultants per unit length and M_x, M_y and M_{xy} are the bending and twisting stress couples per unit length. In addition, the strip stiffness coefficients are defined as

$$(E_{1_{ij}},E_{2_{ij}},E_{3_{ij}})=\int_{-h/2}^{h/2}Q_{ij}(1,z,z^2)\,dz;\qquad i,j=1,2,6 \tag{6}$$

The strain energy per unit volume is $\frac{1}{2}\sigma^T\varepsilon_m$. By using Equations (3) and (4) and integrating with respect to z coordinate through the thickness, the strain energy can be reduced as follows:

$$\begin{aligned}U_s=\frac{1}{2}\iint\Big[&\left\{\varepsilon_l^{\mathrm{T}}[E_1]\;\varepsilon_l-2\varepsilon_l^{\mathrm{T}}[E_2]\;\psi+\psi^{\mathrm{T}}[E_3]\;\psi\right\}\\ &+\left\{2\varepsilon_l^{\mathrm{T}}[E_1]\;\varepsilon_{nl}-2\varepsilon_{nl}^{\mathrm{T}}[E_2]\;\psi\right\}\\ &+\left\{\varepsilon_{nl}^{\mathrm{T}}[E_1]\;\varepsilon_{nl}\right\}\Big]\mathrm{d}x\;\mathrm{d}y\\ +\frac{1}{2}\iiint\Big\{&\varepsilon_T^{\mathrm{T}}[Q]\varepsilon_T-2\varepsilon_l^{\mathrm{T}}[Q]\varepsilon_T-2\varepsilon_{nl}^{\mathrm{T}}[Q]\varepsilon_T+2\psi^{\mathrm{T}}\left(z[Q]\right)\varepsilon_T+\varepsilon_T^{T}[Q]\varepsilon_T\Big\}\,dxdydz\end{aligned} \tag{7}$$

Solution of the non-linear problem is sought through the application of the principle of minimum potential energy. This, of course, requires the assumption of a

displacement field to represent the variations of *u*, *v* and *w* over the middle surfaces. Here, the displacement field adopted for typical finite strip shown in Figure 2 is

$$u = \sum_{i=1}^{ru} U_i(x) g_i^u(y)$$
$$v = \sum_{i=1}^{rv} V_i(x) g_i^v(y) \tag{8}$$
$$w = \sum_{i=1}^{rw} W_i(x) g_i^w(y)$$

where U_i, V_i ,and W_i are trigonometric functions satisfying the kinematic conditions prescribed at the strip ends. In addition, *ru*, *rv* and *rw* represent the number of longitudinal terms assumed for the corresponding displacement functions. The $g_i(y)$ functions are transverse polynomial interpolation functions of various types and orders. The crosswise functions appearing in Equation (8) can be expressed in shape function form, for each longitudinal series term n , as

$$g^u(y) = N_1^u(y).u_1 + N_2^u(y).u_2 + N_3^u(y).u_3$$
$$g^v(y) = N_1^v(y).v_1 + N_2^v(y).v_2 + N_3^v(y).v_3 \tag{9}$$
$$g^w(y) = N_1^w(y).w_1 + N_2^w(y).\theta_1 + N_3^w(y).w_2 + N_4^w(y).\theta_2$$

where $\theta = \partial w/\partial y$ and $N(y)$ are transverse polynomial shape functions. As discussed in Figure 3, the second-order Lagrangian shape function with middle node for u , v and cubic Hermitian polynomials for w are utilized to calculate more accurate results.

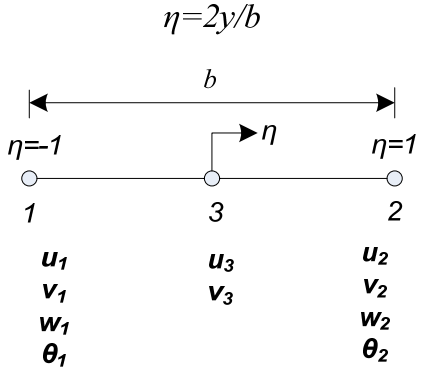

$$N_1^u(\eta) = N_1^v(\eta) = \tfrac{1}{2}(\eta^2 - \eta)$$
$$N_2^u(\eta) = N_2^v(\eta) = \tfrac{1}{2}(\eta^2 + \eta)$$
$$N_3^u(\eta) = N_3^v(\eta) = 1 - \eta^2$$
$$N_1^w(\eta) = \tfrac{1}{4}(2 - 3\eta + \eta^3) \qquad N_2^w(\eta) = \tfrac{1}{8}(1 - \eta - \eta^2 + \eta^3)$$
$$N_3^w(\eta) = \tfrac{1}{4}(2 + 3\eta - \eta^3) \qquad N_4^w(\eta) = \tfrac{1}{8}(-1 - \eta + \eta^2 + \eta^3)$$

Figure 3. Transverse polynomial shape functions for FGS

After some algebraic and matrix manipulation, with the development of the finite strip displacement field according to the above equations, the potential energy of a finite strip can ultimately be expressed in the form

$$U_s = -d^T T_d W + \tfrac{1}{2} d^T \left[K - T_d K^{**} \right] d + \tfrac{1}{6} d^T [K_1] d + \tfrac{1}{12} d^T [K_2] d \qquad (10)$$

where the column matrix d contains the strip degrees of freedom (i.e. d^u, d^v, and d^w) and W is a column matrix of constants. The quantity $T_d = T_c - T_m$ is a variable which is changed, whilst T_m is kept constant throughout the analysis, in order to trace the thermal postbuckling characteristics of the plate. It is noted that K, K^{**}, K_1 and K_2 are symmetric square stiffness matrices. Matrix K and K^{**} are associated with linear behaviour and the effects of the temperature change on stiffness, respectively. Besides, the individual entries of matrix K_1 and K_2 are linear and quadratic functions of the displacements, respectively.

In evaluating the various energy contributions shown in Equation (10), all the integrations are determined analytically.

For the whole plate, comprising an assembly of finite strips, the strain energy is simply the summation of the strain energies of all the individual strips, and correspondingly whole-plate matrices are generated by appropriate summations of strip matrices in the standard fashion. Thus, the potential energy for whole plate can be expressed in the same form as that of Equation (10), as

$$U_s = -\overline{d}^T T_d \overline{W} + \tfrac{1}{2} \overline{d}^T \left[\overline{K} - T_d \overline{K}^{**} \right] \overline{d} + \tfrac{1}{6} \overline{d}^T \left[\overline{K}_1 \right] \overline{d} + \tfrac{1}{12} \overline{d}^T \left[\overline{K}_2 \right] \overline{d} \qquad (11)$$

where the overbar ($\overline{\ }$) indicates a whole plate quantity.

The plate equilibrium equations are obtained by applying the principle of minimum potential energy. In the present study the iterative Newton–Raphson procedure is selected for solving the equations. Once the global equilibrium equations are solved and the nodal degrees of freedom are found for a particular thermal loading, it is possible to calculate the displacements *u*, *v* and *w* at any point in any finite strip using Equation (8), and to determine force and moment quantities through use of Equation (5). Particularly, the average longitudinal force (N_{av}) is determined by integrating the membrane stress resultant (N_x) over the strip middle surface area. Eventually, the total longitudinal force acting on a plate, could be exerted by the summation of such strip end forces as

$$N_{av} = \frac{\sum_{strips} \int_{-b/2}^{b/2} \int_{0}^{A} N_x(x,y)\,dxdy}{A} \qquad (12)$$

3 Numerical Results and Discussion

In this section, various results for thermal postbuckling analysis of rectangular FGM plates are obtained. The performance of the present FSM in solving the thermal postbuckling problem is demonstrated by comparing the results obtained by the current method with those presented in the literature. Subsequently, some more data for FG plates are presented.

3.1 Thermal postbuckling of isotropic plates

A thin isotropic square plate with the following material properties is considered [4]:

$$E = 1 \quad ; \quad A/B = 1 \quad ; \quad A/h = 100 \quad ; \quad \alpha = 1\times10^{-6}\ /^{\circ}C \quad ; \quad \upsilon = 0.25$$

The boundary conditions are assumed to be sliding simply supported (i.e. S3 boundary conditions in Ref [4]); in other words

$$\begin{aligned} u &= w = 0 \ , \quad at \quad x = 0, A \\ v &= w = 0 \ , \quad at \quad y = 0, B \end{aligned}$$

To satisfy the above boundary conditions, the longitudinal functions (i.e. U_i, V_i, W_i) in Equation (8) are selected as sine, cosine, and sine, respectively. The convergence study is examined for two different uniform temperature distribution (i.e. $\Delta T = 135$ and $\Delta T = 280$).

	ΔT=135		*ΔT=280*	
No. of Strips	*W/h*	N_{av}*(N/m)*	*W/h*	N_{av}*(N/m)*
4	0.0674	-0.01769	0.4630	-0.02301
6	0.0726	-0.01765	0.4628	-0.02248
8	0.0715	-0.01766	0.4625	-0.02285
10	0.0715	-0.01766	0.4625	-0.02285

Table 1: Convergence study with regard to the number of strips
(Uniform Temperature Distribution)

According to Table 1, eight finite strips are sufficient to have converged results.
The square plate is subjected to the following temperature distribution called tent-like without external mechanical loading:

$$\begin{aligned} \Delta T(x,y) &= \Delta T_0 + 2.\Delta T_1.\bar{y} && (0 \le \bar{y} \le \frac{1}{2}) \\ &= \Delta T_0 - 2.\Delta T_1.(\bar{y} - 1) && (\frac{1}{2} \le \bar{y} \le 1) \end{aligned} \tag{13}$$

where $\bar{y} = y/B$ and coordinate system origin is located on the plate corner. In Equation (13), ΔT_0 is the uniform temperature rise and ΔT_1 is the temperature gradient; therefore, temperature distribution in y-direction of plate varies from ΔT_0 on the longitudinal edges of plate to the maximum value equivalent to $(\Delta T_0 + \Delta T_1) = \Delta T_2$ at $y = B/2$. It should be noted that by substituting $\Delta T_1 = 0$, the uniform in-plane temperature distribution will be obtained.
It is observed that ΔT_{2cr} (the critical value of ΔT_2) in the tent-like temperature case ($\Delta T_{2cr} = 240.71$) is about 85 percent greater than in the uniform loading case ($\Delta T_{2cr} = 131.53$).

The calculated results are depicted with those from Ref. [4] in Figure 4 and Figure 5.

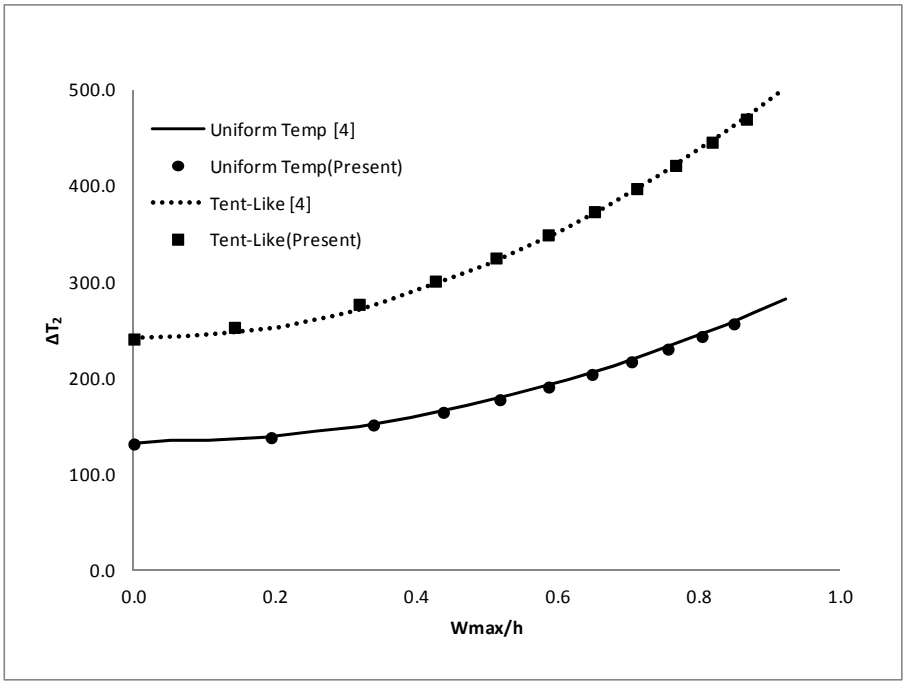

Figure 4. Dimensionless central deflection of plate versus temperature rise

In Figure 4, the tent-like results are calculated for $\Delta T_0/\Delta T_1 = 0.6354$ ($\Delta T_0 = 95.3125$, $\Delta T_1 = 150$). It is clear that the two sets of ΔT_2 versus $w_{\max}/h$ compare very closely to those obtained in previous work.

It is worth mentioning that, whether in the postbuckling or prebuckling regions, the average force N_{av} for a given ΔT_2 is much greater in the uniform temperature case.

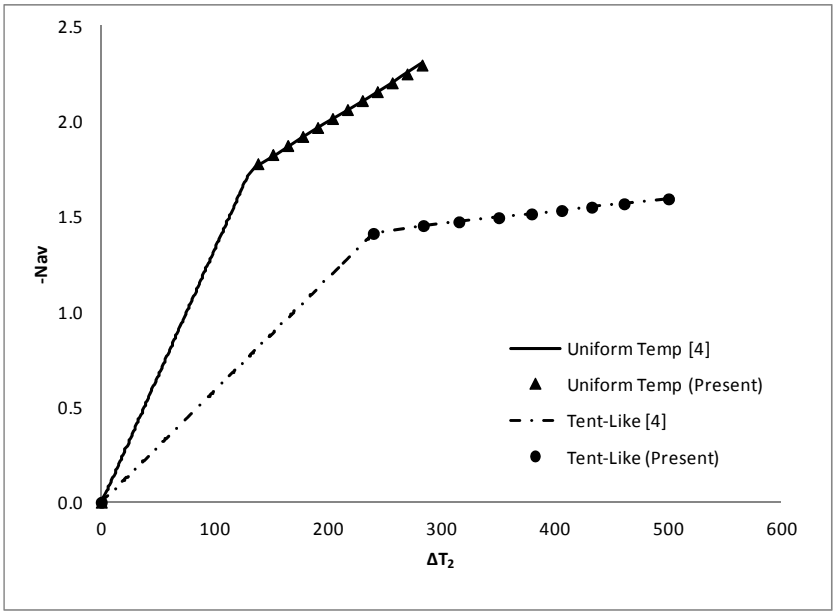

Figure 5. longitudinal force versus variation of temperature rise

3.2 Thermal postbuckling of FGPs

A FG plate made from aluminium (as metal constituent) and alumina (as ceramic constituent) with dimension ratios of $A/B=1$ and $A/h=100$ is considered. The Young's modulus, the thermal expansion coefficient, and the heat conduction coefficient of each material are given as follows:

$$E_c = 380\ GPa \quad , \quad \alpha_c = 7.4\times10^{-6}\ /K \quad , \quad K_c = 10.4\ W/mK$$
$$E_m = 70\ GPa \quad , \quad \alpha_m = 23\times10^{-6}\ /K \quad , \quad K_m = 204\ W/mK$$

Poisson's ratio is assumed to be constant ($\nu = 0.3$) over the entire plate. Similar to that assumed in Ref [4], the boundary conditions on four edges are considered to be S1 fixed simply supported ($u = v = w = 0$). For the first thermal loading, the behaviour of the above plate is investigated while the temperature uniformly increases from reference temperature ($T_{ref} = 300$).

The maximum deflection variation of plate regarding to temperature change is plotted in Figure 6. According to the figure, two sets of data related to aluminium and alumina (fully isotropic and homogenous) reveal clear bifurcation points while other series, which are functionally graded through the thickness, deform by any change in temperature.

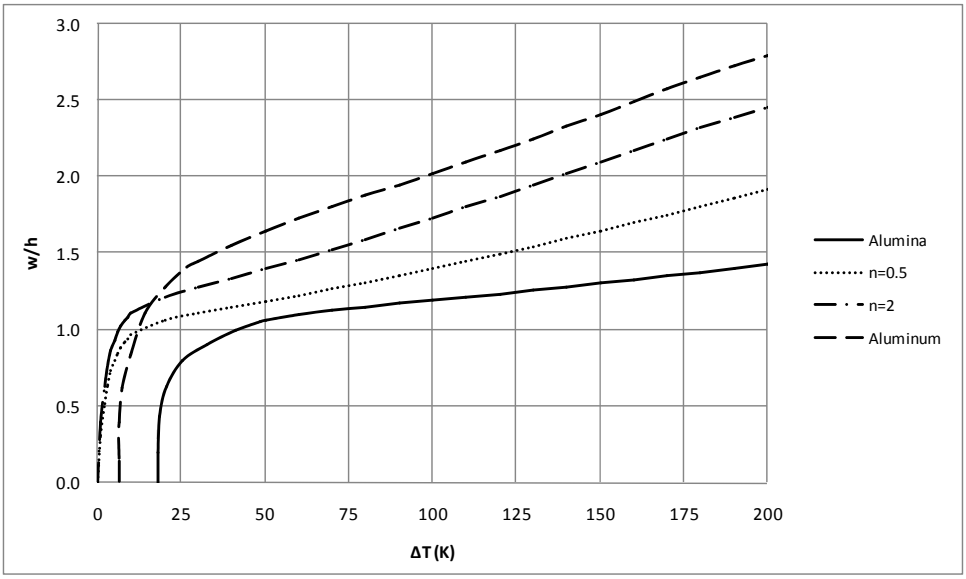

Figure 6. Dimensionless central deflection of the FG plate versus ΔT uniform temperature rise across the thickness

As second thermal loading case, a nonlinear temperature change across the thickness is assumed. The temperature profile is obtained by solving the heat conduction equation for steady-state conditions as:

$$-\frac{d}{dz}\left[K(z)\frac{dT}{dz}\right]=0 \tag{14}$$

By substituting Equation (1) in Equation (14) and considering temperature boundary conditions ($T=T_m$ at $z=-h/2$ and $T=T_c$ at $z=+h/2$) the related heat conduction equation is derived. Two different approaches are used to solve this differential equation, i.e. approximate and exact solutions. In the approximate approach, the differential equation is solved by means of a polynomial series and the approximate temperature distribution across the thickness is selected by taking the first seven terms of the series [7]. In the second approach, Equation (14) is solved analytically. The distribution profiles for each approach are clearly depicted and compared in Figure 7. It is noted that, in the approximate approach, even by taking the first fourteen terms of series (i.e. twice as the number of terms selected before), the results are still surprisingly different from those obtained by the exact solutions.

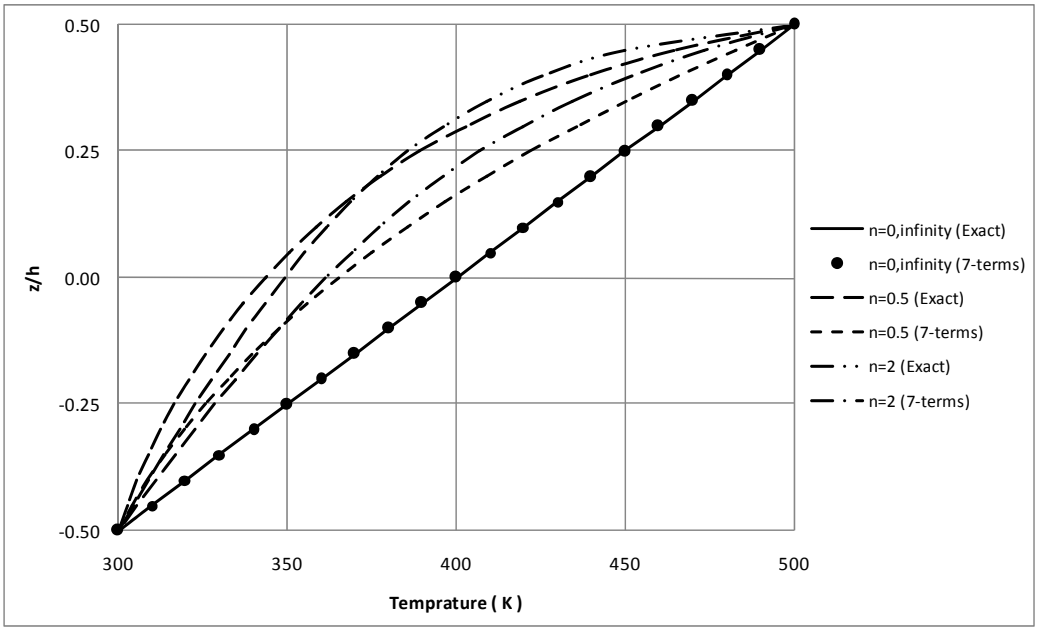

Figure 7. Temperature distribution comparison
for some FG plates across the plate thickness

The data drawn in Figure 8 and 9 are extracted based on the approximate and exact temperature distribution, respectively. In Figure 8 and Figure 9, the maximum dimensionless deflection of some plates under nonlinear temperature change with regards to ΔT_c is shown based on the approximate and exact temperature distributions, respectively. In this loading case, the fully metal surface has a constant temperature value ($T_m = 300\,K$) while fully ceramic surface temperature (T_c) increases monotonously as compared with the reference temperature.

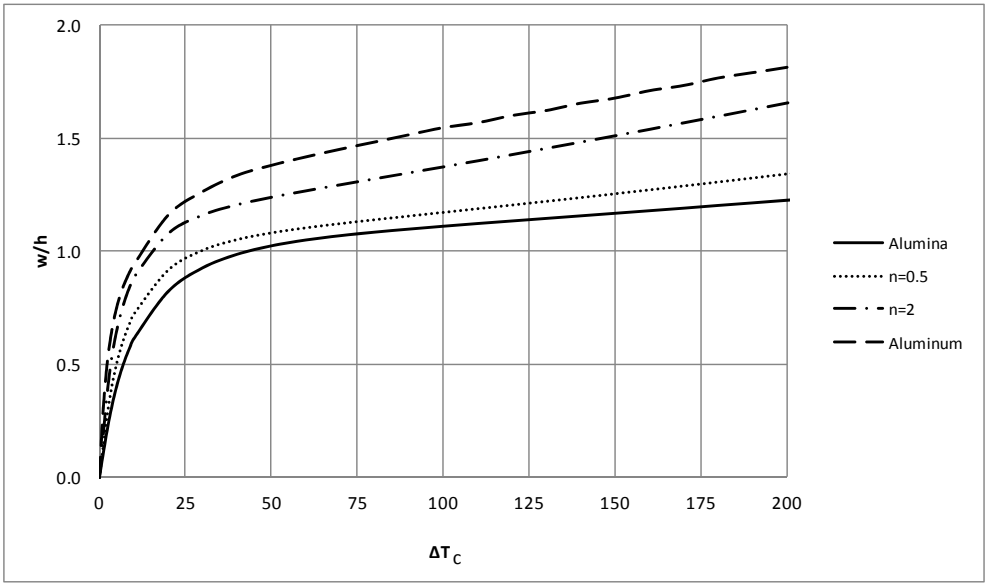

Figure 8. Dimensionless central deflection of the FG plate versus ΔT_c
nonlinear temperature change (approximate temperature distribution)

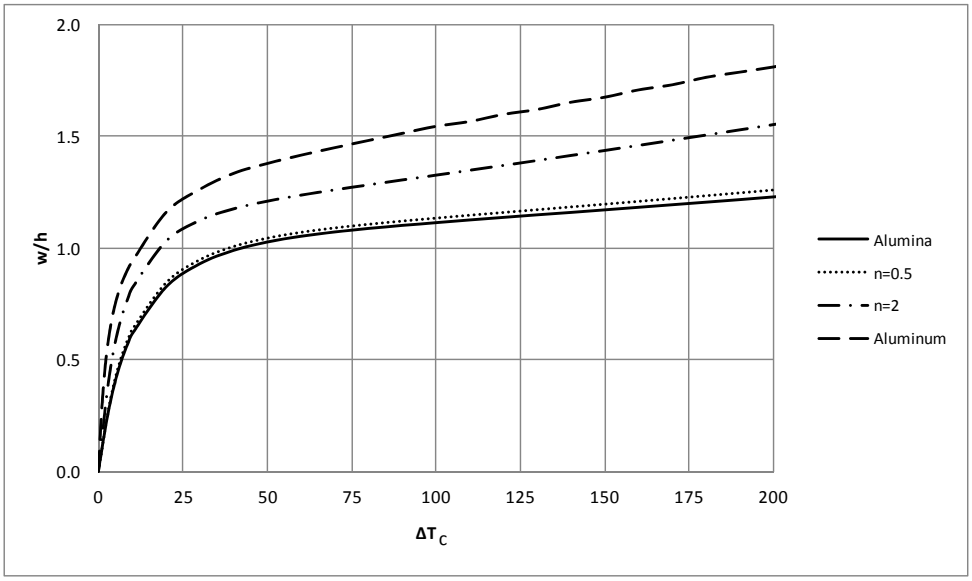

Figure 9. Dimensionless central deflection of the FG plate versus ΔT_c nonlinear temperature change (exact temperature distribution)

Although the isotropic plates (fully made of aluminium or alumina), according to Figure 8 and 9, have the same postbuckling behaviour under nonlinear temperature loadings, whether approximate or exact solution, it is clear that different postbuckling behaviours are obtained for FG plates based on the employed temperature distribution. That is to say that the maximum plate deflection based on the exact temperature distribution is lower than those obtained based on the other distribution. In addition, as volume fraction index is increased, the contained quantity of ceramic decreases. In other words, when volume fraction index n is increased, the central displacement increased. Moreover, the deflection of the plate under uniform temperature rise is greater than that obtained under nonlinear temperature distribution.

4 Conclusions

The application of the FSM is successfully extended to the analysis of postbuckling behaviour of functionally graded plates subjected to thermal loadings.
It is seen that by increasing the volume fraction of ceramic phase, the effects of thermal stresses decreases due to a higher stiffness value of ceramic material.
It can be concluded that FG plates under either uniform or nonlinear temperature change across the thickness show better postbuckling characteristics than homogenous metal plates. In other words, maximum out-of-plane deflection within postbuckling regime is lower than those values corresponding to metal plates.

References

[1] H. R. Ovesy , S. A. M. Ghannadpour, G. Morada, “Post-buckling behavior of composite laminated plates under end shortening and pressure loading, using two versions of finite strip method”, Composite Structures, 75, 106-113 (2006).

[2] H. R. Ovesy , J. Loughlan, S. A. M. Ghannadpour, “Geometric non-linear analysis of channel sections under end shortening, using different versions of the finite strip method”, Computers & Structures, 84, 855-872 (2006).

[3] H. R. Ovesy , S. A. M. Ghannadpour, “An exact finite strip for the initial postbuckling analysis of channel section struts”, Computers & Structures, 89, 1785-1796 (2011).

[4] Y. Ge, W. Yuan, D.J. Dawe, “Thermomechanical postbuckling of composite laminated plates by the spline finite strip method”, Composite Structures,71, 115–129, 2005

[5] K.M. Liew, J. Yang, S. Kitipornchai, “Postbuckling of piezoelectric FGM plates subject to thermo-electro-mechanical loading”, Int. J. of Solids and Structures,40, 3869–3892,2003

[6] K.-J. Sohn, J.-H. Kim, “Structural stability of functionally graded panels subjected to aero-thermal loads”, Composite Structures, 82, 317–325, 2008

[7] S.A.M. Ghannadpour, H.R. Ovesy, M. Nassirnia, “ Buckling analysis of functionally graded plates under thermal loadings using the finite strip method” Computers and Structures J, 2012, doi:10.1016/j.compstruc.2012.02.011